

Thermodynamics of Carbon Monoxide Binding by Helical Hemoprotein Models: the Effect of a Competing Intramolecular Ligand

Kyung-Hoon Lee, Michelle L. Kennedy, Maria Buchalova and David R. Benson*

Department of Chemistry, University of Kansas, Lawrence, KS 66045, USA

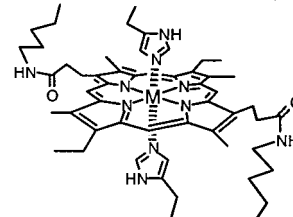
Received 26 February 2000; accepted 5 September 2000

Abstract—Ferrous hemoprotein models **1** and **2** exhibit bis-histidine/mono-histidine coordination equilibrium in aqueous solution. Carbon monoxide binds more tightly to **1** than to **2**, a result of stronger Fe(II)–His coordination in **2** arising from interactions between the Trp side chain and the porphyrin ring. Coordination of the more weakly bound histidine ligands to Fe(II) in **1** is shown to be enthalpically favored but entropically disfavored due to the accompanying change in peptide conformation from random coil to α -helix. We demonstrate that competition from the intramolecular His ligand in **1** reduces ΔH° of CO binding compared to the mono-His coordinated form of the compound, an effect which is largely compensated by the positive entropy term due to unwinding of the peptide helix. Trading enthalpic stabilization of an Fe–ligand bond for an entropy gain due to a protein conformational change may be a common mode of action for hemoproteins which function as small molecule sensors. © 2000 Elsevier Science Ltd. All rights reserved.

Introduction

Binding of diatomic ligands to heme cofactors of hemoproteins is often accompanied by functionally important protein conformational changes. The best understood of these occur upon complexation of O₂ by hemoglobin (Hb).¹ In the hemoprotein FixL, binding of O₂ triggers a conformational change that modulates kinase activity, an important step in regulation of nitrogen fixation.² Loss of the proximal histidine (His) ligand in guanylyl cyclase upon binding of NO is believed to trigger reorganization of the guanosine triphosphate (GTP) binding site and thereby allow conversion of GTP to cyclic GMP.³ Although the majority of hemoproteins that bind exogenous ligands have a single protein-based ligand and the iron is penta-coordinated in the physiologically active state, the recently discovered CO-sensing transcription factor CoxA has a hexacoordinated ferrous heme.⁴ It must therefore release one of its ligands before binding CO. A concomitant conformational change permits the protein to recognize its DNA target.⁴ Herein we report the results of equilibrium CO binding studies with ferrous hemoprotein models **1** and **2**. Like CoxA, **1** and **2** have intramolecular ligands that compete with CO for coordination to iron and also must undergo substantial conformational changes before binding CO.

H₂NCO-A-K-E-A-A-H-A-E-A-X-E-A-A-NHAc



AcNH-A-A-E-X-A-E-A-H-A-A-E-K-A-CONH₂

1: X = Ala, M = Fe(II); **1**⁺: X = Ala, M = Fe(III)
2: X = Trp, M = Fe(II); **2**⁺: X = Trp, M = Fe(III)

The peptides in the ferric forms of **1** and **2** (**1**⁺ and **2**⁺, respectively) exhibit ~50% and ~83% helix content, respectively, in neutral aqueous solution at 281 K as determined by circular dichroism (CD) spectroscopy.^{5,6} ¹H NMR studies of the corresponding diamagnetic Co(III) analogs confirm that the helices in **2**⁺ are more highly organized than in **1**⁺.⁵ The untethered peptides have no regular secondary structure, demonstrating that peptide helicity in **1**⁺ and **2**⁺ requires Fe–His bond formation. The higher helix content in **2**⁺ results from edge-to-face interactions between the tryptophan (Trp) side chains and the porphyrin ring, which also stabilize Fe(III)–His coordination in **2**⁺ relative to **1**⁺ as determined from pH titrations.⁵ In this report we show that Trp also stabilizes Fe(II)–His coordination in **2** relative to **1**. Furthermore, we show that competition from the intramolecular His ligand in **1** exerts a dramatic effect on the relative contributions of enthalpy and entropy for CO binding compared to the corresponding mono-His coordinated compound.

Keywords: peptides and polypeptides; porphyrins and analogs; iron and compounds; complexes; conformation.

* Corresponding author. Tel.: +1-785-864-4090; fax: +1-785-864-5396; e-mail: drb@ukans.edu

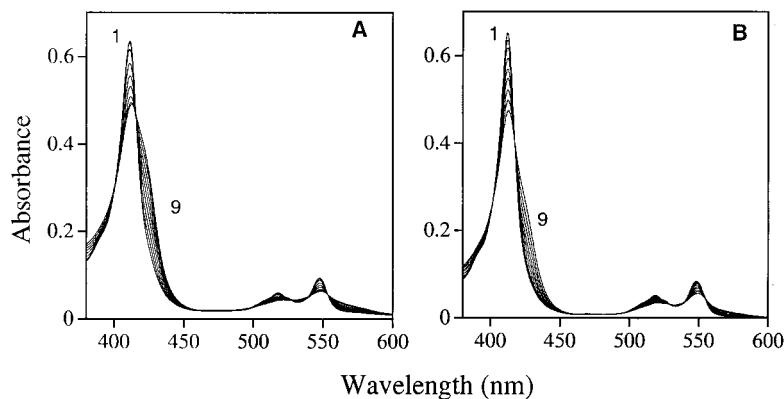


Figure 1. UV/Vis spectra of **1** (A) and **2** (B) as a function of temperature. Spectrum 1, $T=10.9^{\circ}\text{C}$; Spectrum 9= 63.7°C .

Results

Peptide conformation in **1** and **2**

Helix contents for **1**⁺ and **2**⁺ at 297.4 K, the temperature chosen for equilibrium binding studies in the present work, are ~ 36 and $\sim 74\%$, respectively, as determined by CD spectroscopy (data not shown). Unfortunately, CD spectra of the ferrous complexes **1** and **2** could not be recorded due to strong absorbance by sodium dithionite in the far-UV region of the spectrum. However, enhanced peptide helix content in **2** relative to **1** can be inferred by the stronger Fe(II)–His coordination in **2**, discussed in the following section.

Histidine to iron coordination in **1** and **2**

UV/Vis spectra of **1** and **2** over a range of temperatures are shown in Fig. 1. As temperature increases, the Soret band for the bis-His coordinated porphyrin ($\lambda_{\text{max}} \sim 412$ nm) decreases in intensity and a broad peak centered near 420 nm grows in. This new peak is more prominent in the spectra of **1** than of **2** at all temperatures investigated, demonstrating that Fe(II)–His coordination in **2** is stabilized relative to **1**. A number of isosbestic points are observed, suggesting that only two species are involved in the equilibrium. The data indicate that these species are bis-His (low spin) and mono-His (high spin) coordinated Fe(II)

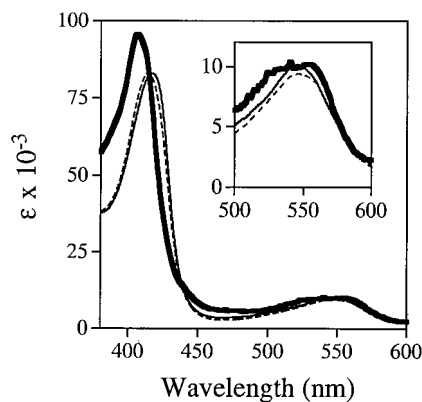


Figure 2. UV/Vis spectra of **3** at 17.7°C (solid line) and 55.7°C (dashed line) at pH 8.0, and at 25°C at pH 6.0 (bold line). All samples were prepared in 1:1 (v/v) $\text{H}_2\text{O}/\text{CH}_3\text{OH}$ with 100 mM buffer (potassium phosphate for pH 8.0, sodium phosphate/citrate buffer for pH 6.0).

porphyrins. Absence of Fe(II)–aquo complexes at equilibrium in **1** and **2** (which would be formed if both intramolecular His ligands were lost) can be demonstrated by comparing the spectra of **3** (the mono-peptide analog of **1**) at pH 8.0 and pH 6.0 (Fig. 2). The Soret band λ_{max} and the shapes of the visible bands at these two pH values are strikingly different. The UV/Vis spectrum of **3** at pH 8 ($\lambda_{\text{max}}=418$ nm) is nearly identical to the spectrum of Traylor's chelated mesoheme (**4**)⁸ in aqueous micelle suspension at pH 7.3 (see Fig. 3 in Ref. [8]). In contrast, the spectrum of **3** at pH 6.0 ($\lambda_{\text{max}}=407$ nm) is essentially the same as that of water-soluble Fe(II) coproporphyrin I (**6**), a reasonable analog of the Fe(II)–aquo complexes of **1** and **2** (Table 1). Furthermore, only minor changes in the spectrum

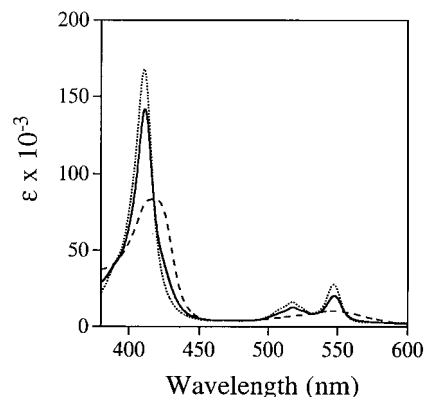


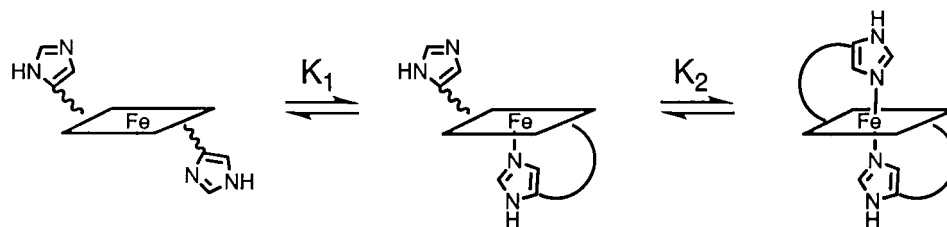
Figure 3. UV/Vis spectra of **1** (solid line), **3** (dashed line) and the bis-imidazole complex of Fe(II)-**7**. All spectra were recorded at 24.7°C in aqueous solution, buffered to pH 8 with 100 mM potassium phosphate.

Table 1. Soret band λ_{max} and ϵ_{max} data at 297.4 K (all data at pH 8.0 in water unless otherwise noted)

Compound	Soret λ_{max} (nm)	Soret ϵ_{max} ($\text{M}^{-1} \text{cm}^{-1}$)
7 ^a	411	163,500
1	411	141,800
2	412	154,800
6	406	102,000
3 (pH 8) ^b	418	83,100
3 (pH 6) ^b	407	95,500
1 -CO	409	205,500
2 -CO	409	205,100

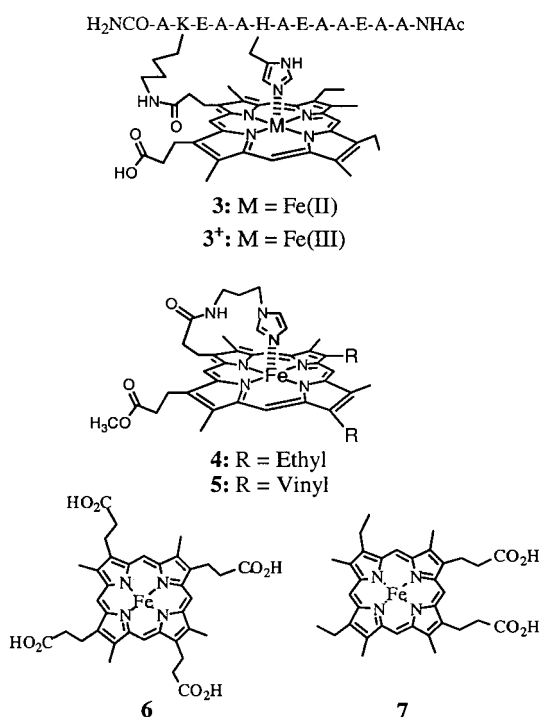
^a In 5 M aqueous imidazole.

^b In 3:1 (v/v) $\text{H}_2\text{O}/\text{CH}_3\text{OH}$.



Scheme 1. Intramolecular Fe(II)–His coordination equilibria in **1** and **2**.

of **3** are observed as temperature is increased (Fig. 2). Taken together, the UV/vis data strongly suggest that at pH 6.0, **3** has lost its His ligand but at pH 8.0 the Fe–His bond is fully intact.⁹ Thus, for both **1** and **2**, $K_1 \gg K_2$ (Scheme 1). This is opposite the typical situation for binding of unhindered imidazole ligands to Fe(II) porphyrins.¹¹



Determining K_2 values for **1** or **2** at a given temperature requires information about the percentage of bis-His and mono-His coordinated forms present at that temperature. As models for the bis-His and mono-His coordinated forms of **1** and **2** we chose Fe(II) mesoporphyrin IX (**7**) in 5 M aqueous imidazole solution and **3** in 1:1 (v/v) CH₃OH/H₂O, respectively. UV/Vis spectra of these complexes (Fig. 3) were summed in various ratios until the best fit to the experimentally observed spectra of **1** and **2** at a particular temperature was obtained. For example, data recorded at 24.4°C indicate that K_2 values for **1** and **2** are 3.0 and ~9, respectively (Table 2). Values of K_2 for **1** measured over a range of temperatures were subsequently used to calculate enthalpies and entropies for Fe–His bond formation ($\Delta H^\circ_{\text{His}}$ and $\Delta S^\circ_{\text{His}}$, respectively) by van't Hoff analysis (Table 2). Values of $\Delta H^\circ_{\text{His}}$ and $\Delta S^\circ_{\text{His}}$ for **2** are not reported, as fits of the data for the model compounds to those of the experimental spectra were not as satisfactory as in the case of **1**. Nonetheless, the available data show that Fe–His bond formation in **2** is also strongly favored by enthalpy and disfavored by entropy.

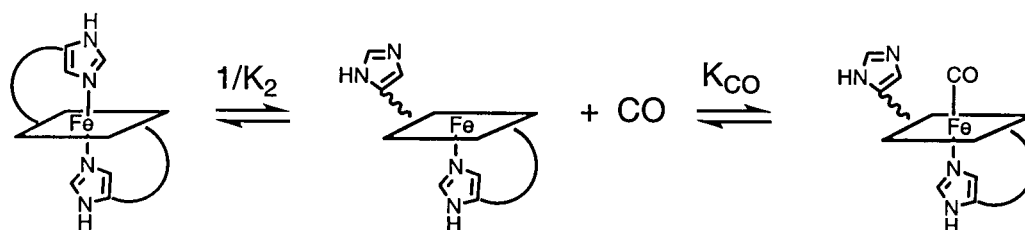
Equilibrium CO binding studies with **1** and **2**

Binding of CO by **1** and **2** competes with coordination of the second (intramolecular) His ligand (Scheme 2). Thus, the equilibrium constant derived from CO binding studies ($K_{\text{app}}^{\text{CO}}$) will be equal to the equilibrium constant for binding of CO to the mono-His coordinated forms of the compounds (K_{CO}) divided by K_2 (Eq. (1)). Values of $K_{\text{app}}^{\text{CO}}$ for **1** and **2** were determined by equilibrium methods in

Table 2. Thermodynamic data for **1** and **2** at 297.4 K in water, pH 8.0

Cpd	K_2	$\Delta G^\circ_{\text{His}}$ (kcal/mol)	$\Delta H^\circ_{\text{His}}$ (kcal/mol)	$\Delta S^\circ_{\text{His}}$ (cal/mol·K)	$K_{\text{app}}^{\text{CO}}$ (M ⁻¹)	$\Delta G^{\circ\text{CO}}_{\text{app}}$ (kcal/mol)	$\Delta H^{\circ\text{CO}}_{\text{app}}$ (kcal/mol)	$\Delta S^{\circ\text{CO}}_{\text{app}}$ (cal/mol·K)
1	3.0	-0.65	-10	-32	3.0×10^7 (0.7) ^a	-10.2	-9.0 (0.6)	4.0 (2.1)
2	~9	~1.3	n.d.	n.d.	1.2×10^7 (0.2)	-9.7	-9.2 (0.4)	1.6 (1.7)

^a Numbers in parentheses represent standard deviations.



Scheme 2. Equilibria involved in CO binding studies with **1** and **2**.

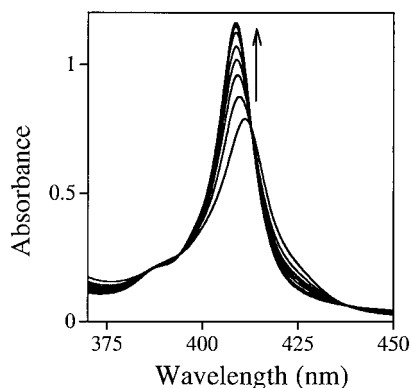


Figure 4. UV/Vis spectra of **1** (5 μM) as a function of CO pressure at 297.4 K.

aqueous solution at pH 8.0 (Table 2), using a previously reported method.¹² Spectra of **1** as a function of CO concentration at 297.4 K are shown in Fig. 4. Taking the $K_{\text{app}}^{\text{CO}}$ and K_2 values determined for **1** and **2** at this temperature and applying Eq. (1), we find that the CO binding affinities (K_{CO}) of the five-coordinated forms of **1** and **2** (K_{CO}) are similar (Table 3).

$$K_{\text{app}}^{\text{CO}} = K_{\text{CO}}/K_2 \quad (1)$$

Values of ΔH° and ΔS° for CO binding by **1** and **2** ($\Delta H_{\text{app}}^{\text{CO}}$ and $\Delta S_{\text{app}}^{\text{CO}}$, respectively), determined by van't Hoff analysis of temperature-dependent equilibrium binding data (Fig. 5), are also reported in Table 2. Approximate values for the enthalpy and entropy for CO binding to the mono-His coordinated form of **1** ($\Delta H_{\text{CO}}^\circ$ and $\Delta S_{\text{CO}}^\circ$, respectively) were calculated from the data in Table 2 (e.g., $\Delta H_{\text{CO}}^\circ = \Delta H_{\text{app}}^{\text{CO}} + \Delta H_{\text{His}}^\circ$) (see Table 3). These data are compared to previously reported data for binding of CO by Mb,¹³ cytochrome P450_{cam}(+)¹⁴ and cytochrome P450_{cam}(-)¹⁴ and Traylor's chelated protoheme (**5**),¹⁵ all determined via kinetic methods. The (+) and (-) for P450_{cam} refer to the presence (+) or absence (-) of the substrate camphor.¹⁴

Discussion

Thermodynamics of Fe–His bond formation in **1** and **2**

One benefit of the relative K_1 and K_2 values in **1** and **2** is that thermodynamic information related to Fe(II)–His bond

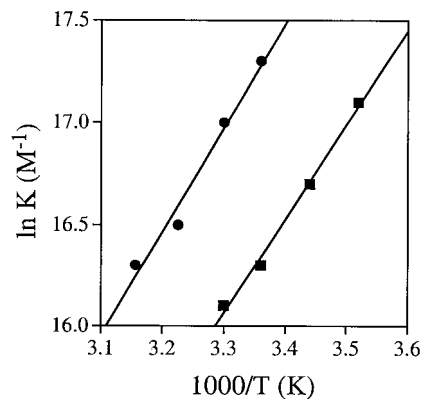


Figure 5. Plots of $K_{\text{app}}^{\text{CO}}$ vs. T^{-1} for **1** (●) and **2** (■). Each point represents the average of at least three measurements. ΔH° and ΔS° were determined from the slope and intercept of these lines, respectively.

formation can be obtained by determining the ratio of mono-His to bis-His coordination (K_2) at a given temperature. As shown in Table 2, the second His ligands in both **1** and **2** are only weakly coordinated. The modestly stronger Fe(II)–His coordination in **2** [$K_2(\mathbf{2})/K_2(\mathbf{1}) \approx 3.0$; $\Delta\Delta G_{\text{His}}^\circ \approx 0.6$ kcal/mol at 297.4 K] results from interactions between the Trp side chain and the porphyrin.

For most Fe(II) porphyrins forming complexes with unhindered imidazole ligands, the association constant for binding of the second ligand is much larger than for the first ($K_2 \gg K_1$; Scheme 1).¹¹ As a result, the mono-coordinated complexes are not normally observed. For sterically hindered ligands such as 2-methylimidazole binding to Fe(II) porphyrins, however, $K_1 \gg K_2$, and it is possible to observe the mono-coordinated species.^{11,16} Traylor and coworkers reported that the second His ligand in **8** (the bis-peptide analog of **4**) is only weakly coordinated in aqueous solution ($K_2 \sim 5$),¹⁷ whereas in **4** (and by analogy in **8**), the first His ligand coordinates much more tightly ($K_1 \sim 800$).⁸ We have previously reported that ferrous hemo-protein models closely related to **1** and **2** also exist as an equilibrium mixture of bis-His and mono-His coordinated forms in aqueous solution.¹⁸ The results presented herein, together with the literature data,^{17,18} suggest that dramatically reduced affinity of Fe(II) for a second intramolecular imidazole ligand relative to the first may be a general phenomenon for Fe(II) porphyrins bearing two intramolecular ligands. The linker attached to each His ligand, regardless of its structure, apparently exerts a significant

Table 3. Thermodynamic data for CO binding at 298 K in water, pH 8.0

Compound	K_{CO} (M^{-1})	$\Delta G_{\text{CO}}^\circ$ (kcal/mol)	$\Delta H_{\text{CO}}^\circ$ (kcal/mol)	$\Delta S_{\text{CO}}^\circ$ (cal/mol K)
1 ^a	9.0×10^7	-10.9	-19	-28
2	$\sim 11 \times 10^7$	~ -11	n.d.	n.d.
5 ^b	3.4×10^8	-11.7 ^f	-17.5	-34
Mb ^c	1.7×10^7	-9.4	-10.7	-4.8
P450 _{cam} (-) ^{d,e}	5.7×10^4	-6.8	13.4	68.0
P450 _{cam} (+) ^{d,e}	2.2×10^4	-6.1	4.1	34.2

^a $K_{\text{CO}} = K_{\text{app}}^{\text{CO}} \cdot K_2$, $K_{\text{app}}^{\text{CO}}$ and K_2 determined at 297.4 K, pH=8.0.

^b In 2% aqueous myristyltrimethylammonium bromide suspension at pH 7.3 (Ref. [15]).

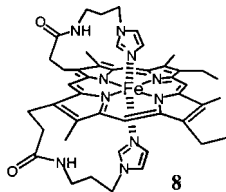
^c Sperm whale Mb at pH 8.5 (Ref. [13]).

^d K_{CO} determined at 293 ± 1 K.

^e Ref. [14].

^f Not reported; calculated from K_{CO} .

pull on the Fe atom, thereby decreasing the affinity of the opposing ligand. Once one ligand has dissociated, the remaining ligand is held tightly in place. It is interesting to compare the effect of the simple linkers on ‘distal’ ligand binding in these model compounds to that induced by the quaternary structure of T-state hemoglobin.¹



Despite the small $\Delta G_{\text{His}}^{\circ}$ for **1**, van't Hoff analysis of temperature-dependent K_2 data shows that coordination of the second His ligand is strongly favored enthalpically. The reason for the very small $\Delta G_{\text{His}}^{\circ}$ is a large, negative $\Delta S_{\text{His}}^{\circ}$. The unfavorable entropy results from the fact that Fe–His bond formation in **1** is accompanied by a large conformational change, the folding of a random coil peptide into an α -helix. Available data reveal that a similar situation holds for **2**.

Thermodynamics of CO binding by **1** and **2**

The equilibrium constants for binding of CO by **1** and **2** ($K_{\text{app}}^{\text{CO}}$, Table 2) are similar to K_{CO} for Mb¹³ (Table 3), despite intramolecular competition for iron by His in the designed hemoproteins. Binding by **1** is stronger than by **2**, although the difference is small [$K_{\text{app}}^{\text{CO}}(\mathbf{1})/K_{\text{app}}^{\text{CO}}(\mathbf{2}) \approx 2.5$; $\Delta \Delta G_{\text{app}}^{\circ} \approx 0.5$ kcal/mol at 297.4 K]. The higher CO affinity of **1** can be attributed almost entirely to weaker bis-His coordination [$K_2(\mathbf{2})/K_2(\mathbf{1}) \approx 3.0$; $\Delta \Delta G_2^{\circ} \approx 0.6$ kcal/mol at 297.4 K], as the values of K_{CO} for **1** and **2** are nearly identical (Table 3).

Van't Hoff analysis of temperature-dependent data (Table 2) reveals that CO binding by **1** and **2** is strongly driven by enthalpy but is also favored by a small, positive entropy term. In contrast, binding by the simpler hemoprotein model **5** is driven entirely by an even more negative enthalpy (Table 3).¹⁵ The $\Delta H_{\text{app}}^{\text{CO}}$ values measured for **1** and **2** represent the difference between the intrinsic enthalpy for binding of CO by the mono-His coordinated forms of the compounds ($\Delta H_{\text{CO}}^{\circ}$) and the enthalpy for intramolecular His coordination ($\Delta H_{\text{His}}^{\circ}$). As shown in Table 2, Fe–CO bond formation by the mono-His coordinated form of **1** is enthalpically favored by about -19 kcal/mol. This is similar to the value of -17.5 kcal/mol measured for **5** by Traylor and coworkers in aqueous micelle solution¹⁵ (Table 3).

From the data discussed in the previous section, we know that Fe(II)–His bond dissociation in **1** and **2** is accompanied by peptide helix unwinding, a process that is highly favored entropically. Thus, the small positive values of $\Delta S_{\text{app}}^{\text{CO}}$ determined for **1** and **2** result from the large negative value of ΔS° for binding of CO by the mono-His coordinated forms of **1** (and by analogy in **2**) (ΔS_{CO} ; Table 3). As with ΔH_{CO} , the value calculated for ΔS_{CO} of **1** is very similar to that reported for **5**. Thus, once the effect of the competing ligand has been taken into account, we find that the intrinsic entropies and

enthalpies for CO binding by **1** and **5** are very similar. This demonstrates that the thermodynamics of CO binding by Fe(II) porphyrins bearing single, unstrained imidazole ligands are not significantly affected by the nature of the linker connecting the ligand to the porphyrin.

Entropic contributions to CO binding in aqueous solution

As noted by Page and Jencks,¹⁹ entropy changes due to losses of translational and rotational degrees of freedom for many simple bimolecular reactions in solution are in the range of -40 – -50 eu. Thus, the relatively large, negative ΔS_{CO} values determined herein for **1** and reported previously for **5** are reasonable. Additional factors can contribute to ΔS_{CO} as well. For example, complete desolvation of CO prior to binding will occur with an entropy change of about $+31$ eu, as estimated from the partial molar entropy of CO in water.^{14,20} For **1,2** and **5**, CO will not be completely desolvated upon binding to Fe(II) but the extent of desolvation should be similar in each case and the effect will be to make the entropy of reaction less negative. Additional modulation of the reaction entropy may arise from restricted rotation of the His ligand about the Fe–His bond, resulting from closer approach of the ligand to the porphyrin as the iron atom moves into the porphyrin plane in the CO complex.

Conclusion

A number of hemoproteins have been discovered in which binding of a diatomic ligand is coupled to a change in protein conformation, with or without loss of a protein-based ligand.^{1–4} Herein, we have shown that CO competes with an intramolecular His ligand for coordination to Fe(II) in **1** and **2**, similar to the situation observed for the transcription factor CooA. Although the intramolecular His ligand reduces the enthalpy of CO binding relative to mono-His coordinated analogs of **1** and **2**, the helix unwinding which accompanies CO binding largely compensates by providing a positive entropy of reaction. Trading enthalpic stabilization of an Fe–ligand bond for an entropy gain due to a protein conformational change, as has been shown to occur in these model compounds, may represent a common mode of action for hemoproteins which function as small molecule sensors.

Experimental

Materials

Syntheses of **1–3** have been reported.^{5,18} All reagents used in this work were of analytical grade or better, and all solvents were degassed prior to use. Carbon monoxide and nitrogen gases were passed through chromous chloride solution to remove dioxygen. Solutions of **1** and **2** buffered at pH 8 were freshly prepared by reduction of the ferric complexes with sodium dithionite in a glove box under a nitrogen atmosphere. Concentrations of **1** and **2** were typically in the range $(4\text{--}6) \times 10^{-6}$ M. Gas saturation was achieved by bubbling the desired gas mixture through the

solution. The solubilities of carbon monoxide in aqueous solution used in our calculations were 1.250 mM at 10.9°C, 1.103 mM at 17.9°C, 0.941 mM at 24.4°C, 0.870 mM at 30.2°C, 0.799 mM at 36.9°C and 0.765 mM at 43.7°C.²¹

Circular dichroism spectroscopy

CD spectra of **1**⁺ and **2**⁺ were recorded on a JASCO 710 circular dichroism spectropolarimeter. The instrument is automatically calibrated with (1S)-(+)-10-camphosulfonic acid. Temperature control was achieved using a circulating water bath. Cell path length (*l*) was 1.0 cm. Concentrations of **1** and **2** were determined by UV/Vis spectroscopy, using the previously determined extinction coefficient at the Soret λ_{\max} of 130,000 M⁻¹ cm⁻¹.⁵ Equations used for calculating helix contents are detailed in Ref. [5].

Measurement of extinction coefficients

UV/Vis spectra were recorded on Kontron UVIKON 9410 or Varian Cary spectrophotometers with thermostated cell compartments. Cuvettes with a 1.0 cm path length were employed. Soret band data are reported in Table 1. Extinction coefficients at the Soret band λ_{\max} of **1**⁺ and **2**⁺ were previously reported to be 130,000 M⁻¹ cm⁻¹ in neutral aqueous solution.⁵ Extinction coefficients for **1** and **2** (50 mM potassium phosphate, pH 8.0) were determined from UV/vis spectra recorded after sodium dithionite reduction of **1**⁺ and **2**⁺ at known concentrations. Extinction coefficients for Fe(II) mesoporphyrin IX and Fe(II) coproporphyrin I in the presence of a saturating concentration of imidazole (5 M) were determined in an analogous manner, using $\epsilon=130,000$ M⁻¹ cm⁻¹ for the Fe(III) complexes. Using the measured ϵ values for **1** and **2**, we determined ϵ for the CO complexes of each from spectra recorded at saturating concentrations of CO. These values were subsequently used to measure ϵ for **3** (Table 1). Specifically, the UV/vis spectrum of **3** (in 1:1 CH₃OH/H₂O, pH 8, to avoid self-association), was recorded following sodium dithionite reduction of solutions of **3**⁺ at an unknown concentration. Concentration of the sample was determined following formation of the CO complex, using ϵ for the CO complexes of **1** and **2**. Extinction coefficients for the Fe(II) coproporphyrin I-aquo complex at pH 8.0 and of **3** at pH 5.0 were determined following sodium dithionite reduction of solutions of the Fe(III) complexes, prepared from a stock solution of known concentration.

Equilibrium CO binding measurements

Equilibrium constants for CO binding ($K_{\text{app}}^{\text{CO}}$) were determined by spectrophotometric titrations.¹² Absorbance changes in the spectral region from 200 to 600 nm were recorded using a Varian Cary spectrophotometer. Treatment of the collected data was carried out using least squares fitting routines. Solutions of the complexes were placed in a gas tight quartz cell of 1.0 cm path length and equilibrated to the desired temperature within an uncertainty of 0.3°C. Temperature was controlled using a thermostated cuvette holder connected to a circulating water bath. Carbon monoxide and nitrogen gasses of known composition were generated

with use of Tylan TO-28 controller with model FC-260 mass flow controllers and compressed gas cylinders.

Acknowledgements

We thank Professor Daryle H. Busch for use of his group's gas mixing apparatus and Professor Kenton R. Rodgers for valuable discussions and suggestions. This work was supported by NIH grant R29-GM52431.

References

- Perutz, M. F.; Wilkinson, A. J.; Paoli, M.; Dodson, G. G. *Annu. Rev. Biophys. Biomol. Struct.* **1998**, *27*, 1.
- (a) Gong, W.; Hao, B.; Mansy, S. S.; Gonzalez, G.; Gilles-Gonzalez, M. A.; Chan, M. K. *Proc. Natl. Acad. Sci. USA* **1998**, *95*, 15177. (b) Rodgers, K. R.; Lukat-Rodgers, G. S.; Tang, L. *J. Am. Chem. Soc.* **1999**, *121*, 11241.
- Zhao, Y.; Hoganson, C. W.; Babcock, G. T.; Marletta, M. A. *Biochemistry* **1998**, *37*, 12458 and references therein.
- Shelver, D.; Thorsteinsson, M. V.; Kerby, R. L.; Chung, S.-Y.; Roberts, G. P.; Reynolds, M. F.; Parks, R. B.; Burstyn, J. N. *Biochemistry* **1999**, *38*, 2669 and references therein.
- Liu, D.; Williamson, D. A.; Kennedy, M. L.; Williams, T. D.; Morton, M. M.; Benson, D. R. *J. Am. Chem. Soc.* **1999**, *121*, 11798. (Compounds **1**⁺ and **2**⁺ are numbered **1** and **3**, respectively, in Ref. [5]).
- Helix content refers to the percentage of amino acids occupying helical conformations averaged over the entire length of the peptide. In reality, helicity is not evenly distributed throughout the sequence, but tends to be higher near the center of the peptide.⁷
- Chakrabarty, A.; Baldwin, R. L. *Adv. Protein Chem.* **1995**, *46*, 141.
- Geibel, J.; Cannon, J.; Campbell, D.; Traylor, T. G. *J. Am. Chem. Soc.* **1975**, *100*, 3575.
- UV/Vis spectra of Fe(II) MPIX and related analogs are highly dependent on the presence or absence of a fifth axial ligand, as well as on the nature of the ligand. In the absence of a fifth ligand, distinct α and β bands are observed and the Soret λ_{\max} is near 400 nm.¹⁰
- Traylor, T. G.; Koga, N.; Deardurff, L. A. *J. Am. Chem. Soc.* **1985**, *107*, 6504.
- Reviewed in: Walker, F. A.; Simonis, U. Iron Porphyrin Chemistry. In *Encyclopedia of Inorganic Chemistry*; King, R. B. Ed.; Wiley: Chichester, 1994; Vol. 4, p 1785.
- Buchalova, M.; Warburton, P. R.; van Eldik, R.; Busch, D. H. *J. Am. Chem. Soc.* **1997**, *119*, 5867.
- Projahn, H.-D.; van Eldik, R. *Inorg. Chem.* **1991**, *30*, 3288.
- Kato, M.; Makino, R.; Iizuka, T. *Biochim. Biophys. Acta.* **1995**, *1246*, 178.
- (a) Traylor, T. G.; Berzinis, A. P. *Proc. Natl. Acad. Sci., USA* **1980**, *77*, 3171. (b) Traylor, T. G. *Acc. Chem. Res.* **1981**, *14*, 102.
- (a) Collman, J. P.; Reed, C. A. *J. Am. Chem. Soc.* **1973**, *95*, 2048. (b) Brault, D.; Rougee, M. *Biochem. Biophys. Res. Commun.* **1974**, *57*, 654. (c) Wagner, G. C.; Kassner, R. *J. Biochim. Biophys. Acta* **1975**, *392*, 319.
- Geibel, J.; Chang, C. K.; Traylor, T. G. *J. Am. Chem. Soc.* **1975**, *97*, 5924. See also Lopez, M. A.; Ybarra, C. D.; Hyatt, S. *Inorg. Chim. Acta.* **1995**, *231*, 121.
- Arnold, P. A.; Benson, D. R.; Brink, D. J.; Hendrich, M. P.;

Jas, G. S.; Kennedy, M. L.; Petasis, D. T.; Wang, M. *Inorg. Chem.* **1997**, *36*, 5306.
19. Page, M. I.; Jencks, W. P. *Proc. Natl. Acad. Sci. USA* **1971**, *68*, 1678.

20. Estimated from its partial molar entropy in water: Wilhelm, E.; Battino, R.; Wilcock, J. R. *Chem. Rev.* **1977**, *77*, 219.
21. Cargill, R. W., Ed. *Solubility Data Series*; Pergamon: Oxford, 1990; Vol. 43.